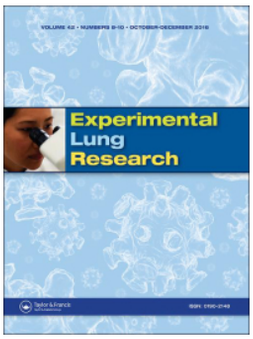

Taylor & Francis
Taylor & Francis Group

Experimental Lung Research

ISSN: 0190-2148 (Print) 1521-0499 (Online) Journal homepage: www.tandfonline.com/journals/ielu20

Artificial stone dust affects oxidative stress and epithelial barrier in CALU 3 cells

Noa Ophir, Elizabeth Fireman, Mordechai Reuven Kramer & Rafi Korenstein

To cite this article: Noa Ophir, Elizabeth Fireman, Mordechai Reuven Kramer & Rafi Korenstein (2025) Artificial stone dust affects oxidative stress and epithelial barrier in CALU 3 cells, Experimental Lung Research, 51:1, 81-90, DOI: 10.1080/01902148.2025.2567064

To link to this article: https://doi.org/10.1080/01902148.2025.2567064

Published online: 06 Oct 2025.

EXPERIMENTAL LUNG RESEARCH
2025, VOL. 51, NO. 1, 81–90
https://doi.org/10.1080/01902148.2025.2567064

Taylor & Francis
Taylor & Francis Group

Artificial stone dust affects oxidative stress and epithelial barrier in CALU 3 cells

Noa Ophir[a,b], Elizabeth Fireman[a,b,c], Mordechai Reuven Kramer[b,d] and Rafi Korenstein[b,e]

[a]Laboratory for Pulmonary and Allergic Diseases, Tel Aviv Medical Center; [b]Gray Faculty of Medical & Health Sciences, Tel Aviv University, Tel Aviv, Israel; [c]Department of Occupational and Environmental Health; [d]Institute of Pulmonary Diseases Rabin Medical Centre; [e]Physiology Pharmacology Department

ABSTRACT

Aim: Artificial Stone Dust (ASD) exposure has been identified as a significant health risk for workers, leading to oxidative stress, inflammatory responses, and potential systemic autoimmune diseases due to its high crystalline silica content. The aim of this study is to identify the impact of ASD on the permeability of alveolar epithelial cells and the mechanisms underlying particle translocation across the alveolar membrane remain unexplored. **Methods**: The acute toxicological effects of ASD on human bronchial submucosal gland cells CALU-3 cells *in vitro* were investigated to assess its impact on epithelial barrier integrity, in comparison to crystalline silica particles (Min-U-Sil®5). **Results:** Exposure to ASD increased oxidative stress, evidenced by heightened Reactive Oxygen Species (ROS) levels and Heme Oxygenase-1 (HO-1) gene expression in CALU-3 cells, exceeding effects observed with Min-U-Sil®5. Notably, ASD exposure resulted in a significant decrease in Transepithelial Electrical Resistance (TEER), indicating compromised epithelial barrier integrity, especially at higher concentrations (3.7 mg,18.5 mg and 37 mg) after 24, 48 and 72 h. These findings were not paralleled by a decrease in cell viability, underscoring a specific effect on cellular barrier function rather than cytotoxicity. **Conclusions:** Our study reveals that ASD induces oxidative stress and disrupts epithelial barrier integrity *in vitro*, potentially contributing to systemic translocation of particles and subsequent health effects. These findings underscore the need for a rigorous protective measure for workers and highlight potential biomarkers of ASD-induced cellular damage.

ARTICLE HISTORY
Received 20 December 2024
Accepted 22 September 2025

KEYWORDS
Artificial Stone Induced Silicosis; CALU-3; Transepithelial Electrical Resistence

Introduction

Inhaled respirable crystalline silica particles are able to reach the alveoli, inducing oxidative stress and inflammatory response that involves alveolar epithelial cells and elements of the immune system.[1] In recent decades the manufacturing and processing of artificial stone has been reported as a possible source of exposure to high levels of crystalline silica in workers.[2]

This specific type of material has become increasingly popular, and it has been largely employed for the production and manufacturing of kitchen and bathroom countertops. Its silica content is approximately 90%, much higher percentage than the silica content of natural marble (3%) or granite stones (30%).[3] Apart from crystalline silica content we and others gave much consideration to non-siliceous components such as resins and metals that may modify chemical interactions and disease risk.[4–6]

We had previously screened exposed workers to ASD by quantitative biometric monitoring of functional and inflammatory parameters showing that this population showed advanced inflammatory and functional deterioration as the result of continuing exposure to ASD.[7]

CONTACT Prof. Elizabeth Fireman, PhD efireman@tauex.tau.ac.il; lizifire@gmail.com Telephone: +972-52-4266901 Department of Occupational and Environmental Health, Sackler School of Medicine Tel Aviv University- ISRAEL; Gray Faculty of Medical & Health Sciences Tel Aviv University- ISRAEL.

In a separate investigation conducted at a lung transplantation center specializing in advanced silica-related lung disease in Israel, we documented an outbreak of autoimmune disorders among a cohort of patients diagnosed with silicosis, specifically associated with exposure to artificial stone materials.[8] The two observations strongly indicate that the inflammatory conditions observed in workers exposed to artificial stone extend beyond the pulmonary system alone. This implies the presence of a mechanism by which particles can exit the lungs and enter circulation, potentially contributing to adverse effects and systemic diseases.

In general, the adverse effects of inhaled particles on damaged tissue for histological and molecular analysis pose practical and ethical challenges. To overcome these limitations many studies and supplementing investigations are focused on studies using Ambient Suspended dust (ASD) and integrating *in vitro* high throughput screening (HTS) essays.[9,10]

Research studies have successfully developed and implemented various *in vivo* animal models to investigate the pathogenesis and molecular basis of silicosis, facilitating the exploration of potential treatments. Among these models, the zebrafish has emerged as an optimal complement to other animal models.[11] However, it is noteworthy that none of these studies have exposed animals to artificial stone dust.

In vitro models serve as the initial layer in toxicological assessments, focusing on elucidating underlying cellular toxic mechanisms. They are frequently employed to predict and extrapolate potential effects to the *in vivo* domain. In a recent publication, human alveolar epithelial cells and macrophages were exposed to engineered dust to evaluate cytotoxicity and inflammation. The study revealed that particle chemistry significantly influences the response of lung cells, emphasizing its crucial role in determining the outcomes.[12]

Trans-epithelial/endothelial electrical resistance (TEER) is a noninvasive and quick method of assessing the integrity of barrier tissues and is used under various conditions.[13] Its efficacy and safety was used to edge-to-edge repair of mitral regurgitation in high-risk patients.[14] In drug permeability studies, the integrity of the monolayer is confirmed by stable TEER readings. Once this is established, drugs are applied, and their permeability is measured by tracking the passage of the drug across the monolayer over time.[15]

To the best of our knowledge, no *in vitro* model using TEER in CALU-3 cells has demonstrated the effect of artificial stone dust on the permeability of alveolar epithelial cells or elucidating the mechanisms underlying the translocation of particles across the alveolar membrane.

In this study, our objective is to compare the in-vitro acute toxicological effects of micrometer-size particles of ASD (amorphous silica dust) with those of pure quartz, which serves as a reference material. Our primary focus is to assess the impact on lung cell function, aiming to characterize short-term molecular changes associated with toxicity pathways.

Additionally, it's crucial to acknowledge the absence of experimental data specifically addressing the mechanisms by which ASD particles traverse the alveolar membrane, potentially culminating in the onset of systemic autoimmune diseases.

Material and methods

Qualitative analysis of artificial stone dust

The working concentrations were estimated based on the approximate average concentration of particles inhaled by the workers, as measured using the Nanosight LM20 instrument. The total sample weight was calculated according to particle size and its relative proportion in the sample, using the following steps:

1. **Particle weight** = particle volume × particle specific density × particle concentration
2. **Weighted particle contribution** = particle weight × particle concentration
3. **Total sample weight** = sum of all weighted particle contributions (step 2)

The weight calculated for the control group was subtracted from the expected weight in marble workers' sputum. This difference was defined as the maximal concentration for use in the *in vitro*

experiments (37 mg/cm^2). Additionally, lower concentrations of 18.5 mg/cm^2 and 3.7 mg/cm^2 were tested to evaluate relative effects.

Morphological observations of ASD particles were conducted using Energy-Dispersive X-ray Spectroscopy (EDS) on a JEOL 840 Scanning Electron Microscope (SEM) equipped with a Link 10,000 system. Dust collection was carried out *via* direct air sampling using a cyclone sampler, and sample preparation was performed according to the manufacturer's instructions.[16]

Crystalline silica particles, Min-U-Sil®5 were used as a reference material (provided by U.S. Silica Co., Berkeley Springs, WV, US).

CALU-3 cell culture cells viability

CALU-3 cell line (American Type Culture Collection, ATCC, HTB-55) derived from human bronchial submucosal glands was used for in-vitro experiments. Cells were cultured at 37 °C and 5% CO2 in Dulbecco's modified Eagle medium (DMEM) (30-2002, ATCC) supplemented with 10% fetal calf serum (FCS), 500units/ml penicillin, and 50 µg/ml streptomycin. CALU-3 cells were grown in 25 cm^2 tissue culture flasks and split when 90% to 95% confluent.

CALU-3 cell viability by Alamar blue assay was tested after 3-24 h exposure to the following concentrations: 37 mg (115mg/cm^2), 18.5 mg (57.5 mg/cm^2) and 3.7 mg (11.5 mg/cm^2) of ASD or Min-U-Sil®5. Chloropromazin (CPM) 65 µM was used as positive control.

Oxidative stress in CALU-3 cells

The production of ROS was measured using 2′,7′-Dichlorodihydrofluorescein diacetate (DCFH-DA, sigma D6883). DCFH-DA passively enters the cells, then cellular esterases act on the molecule to form the non-fluorescent moiety DCFH, which is ionic in nature and, therefore, trapped inside the cell. A reaction with ROS leads to an oxidation of DCFH to the highly fluorescent compound dichloroflourescein (DCF), so the intensity of fluorescence is proportional to intracellular ROS levels. 5 × 105 cells grown in 96-well plates for 10 days, then DCFH-DA was added to the cells for 30 min before the addition of ASD, Min-U-Sil®5, or the positive control 1 mM TBPH. Cells were then washed once with PBS and incubated with ASD or Min-U-Sil®5 particles (3.7, 18.5, 37 mg/cm2) for additional 3 h. A positive control tetrabutylperoxyhydroxide (TBPH, 1 mM) was added for 5 min as well. Intracellular ROS levels were determined by a flow cytometry (CytoFLEX S Blue-Red-Violet-Yellow (2000-2025 B-R-V-Y Beckman Coulter).

RNA extraction and quantitative real-time polymerase chain reaction (RT-PCR) for HO-1 in CALU-3 cells

RNA extraction was done from cultures of CALU-3 cells by SV Total RNA Isolation System (z3101, promega). Quantification of the RNA amount was done by NanoDrop one™ Spectrophotometer (Thermo Scientific). Quantitative Real-Time Polymerase Chain Reaction (RT-PCR) for HO-1, Gene Expression was performed on CALU-3 Cells

For gene expression analyses, quantitative RT-PCR was performed using a Step One Plus Real Time PCR System (Applied Biosystems). For the amplification reactions, the TaqMan Gene Expression Master Mix and Gene Expression Assay kits from Applied Biosystems were used (assay; HO-1: Hs00174097-m1; and GAPDH: Hs99999905-m1). The standard PCR conditions were 10 min at 95 °C, followed by 40 cycles at 95 °C for 15 s and 60 °C for 1 min. The expression levels of the target transcripts in each sample were calculated by the comparative cycle threshold (C t) method (2 – ΔCt formula) after normalization to the glyceraldehyde-3-phosphate dehydrogenase (GAPDH) housekeeping gene.

Transepithelial electrical resistance (TEER) Analysis upon particle exposure

CALU-3 cells were seeded at 5*103 cells/ml in 24-well Transwell inserts (0.4 µm pore size polyester membrane, MCHT24H48, Mercury) with 0.1 ml of media on the apical side and 0.6 ml of media on

the basolateral side. The TEER responses of the cells were measured 30 min after medium changes. After the TEER values reached 500 Ω cm^2 (indicating a confluent monolayer), the cells were exposed to 3.7, 18.5, 37 mg/cm^2 of ASD or Min-U-Sil®5 particles. TEER values were then recorded after exposure up to 72 h after particle treatment. The resistance of each well was calculated by: Ω actual = Ω sample - Ω blank, where Ω sample is the average measurement from a seeded well and Ω blank is the average measurement from wells containing inserts and medium, but no cells. Then, the unit area resistance was calculated by: Ω actual × effective membrane area = Ω × cm^2, where the effective membrane area is 0.33 cm^2 for 24-well Transwell inserts.

Statistical analysis

Comparisons between groups were performed using several statistical tests, selected based on the distribution and nature of the data. The independent t-test was applied to compare the means of two independent groups with normally distributed data to evaluate the effects of ASD and Min-U-Sil®5 on cell viability and oxidative stress levels. In cases where data were non-normally distributed, the Mann-Whitney test was used to assess differences in gene expression levels of HO-1, between the ASD and Min-U-Sil®5 treated groups.

For comparisons involving more than two groups with non-normally distributed data, the Kruskal-Wallis's test was employed. This test was used to analyze differences in TEER values across multiple concentrations of ASD and Min-U-Sil®5 at 24, 48, and 72 h. The Chi-square test was utilized to examine the association between categorical variables, specifically assessing the relationship between particle size distribution and the type of dust (ASD vs. Min-U-Sil®5). Additionally, Spearman correlation analysis was performed to evaluate the relationship between particle concentration and ROS levels when the data did not meet the assumptions for parametric testing.

All statistical analyses were conducted using SPSS software version 24.0 for Windows (Chicago, IL, USA), with a p-value < 0.05 considered statistically significant.

Results

We first analyzed ASD and Min-U-Sil®5 by SEM to visualize its shape and size. Min-U-Sil®5 was characterized by smaller particles up to 5 µm whereas ASD, collected directly from the air using cyclone sampler while cutting artificial stone surface. Both showed crystalline shapes (Figure 1a,b). 90% of ASD particles were <6 µm, and 99% of Min-U-Sil®5 were <6 µm (Figure 1c).

Then we assessed CALU-3 cell viability by Alamar blue assay after 3- and 24-h exposure to stimulate acute exposure to the following concentrations:" 37 mg (115 mg/cm^2), 18.5 mg (57.5 mg/cm^2) and 3.7 mg (11.5 mg/cm^2) of ASD or Min-U-Sil®5. Chlorpromazine (CPM) 65 µM was used as positive control and cause death of the cells after 3 h. No significant difference in cell viability was observed in the cells exposed to ASD or Min-U-Sil®5 at different time points or relative to the unexposed control (Figure 2a–c)

Oxidative stress was first assessed by an optical probe, DCFH-DA, treating the CALU-3 cell with an increase concentration- of ASD vs Min-U-Sil®5. In fact, DCF fluorescence was significantly higher in cells stimulated by ASD compared to reference material and positive control (Figure 3). DCF fluorescence intensity was measured at 485 nm excitation and 530 nm emission and the results were expressed relatively to control (unexposed cells) ± SD of three independent experiments.

Subsequently we study the transcription of HO-1 in CALU-3 cells by exposure to ASD and Min-U-Sil®5 was tested after 3 and 24 h of exposure, A significant HO-1 increase in transcript levels, a was observed after exposure to ASD compared with Min-U-Sil®5 being the highest dose of 37 mg after 3 h (Figure 4a) and after 24 h (Figure 4b), regardless of the treatment concentration. Min-U-Sil®5 did not change transcript levels compared to control.

The effect of increasing concentrations of ASD and Min-U-Sil®5 on the epithelial barrier integrity was monitored after 24, 48 and 72h of exposure. Results showed a statistically significant decrease in TEER after 48 h and 72 h incubation with 18.5 mg and 37 mg of ASD relative to Min-U-Sil®5 (Figure 5a–c).

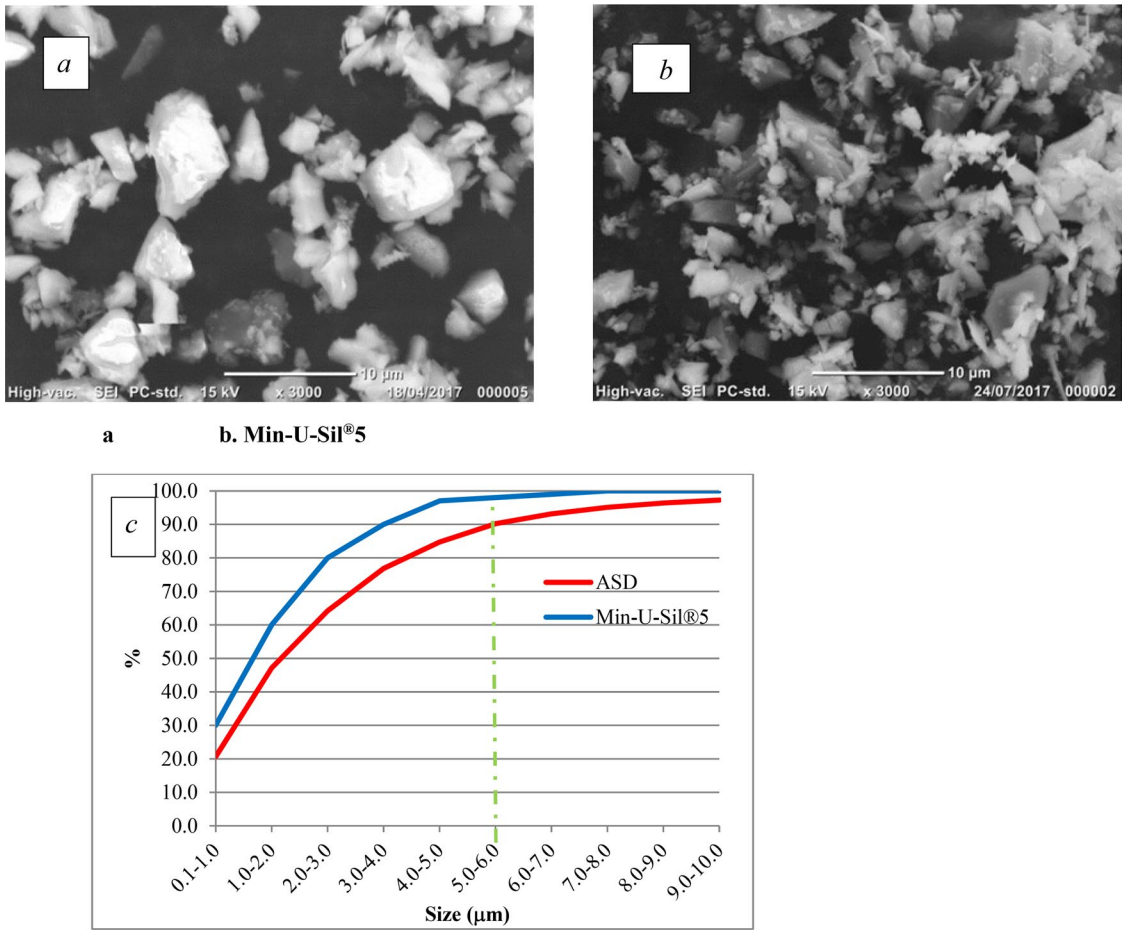

Figure 1. SEM images of (a) ASD, (b) Min-U-Sil®5 and (c) particles size distribution.
The samples were collected and prepared as described in MATERIAL and METHODS
a SEM images of ASD artificial stone dust b Min-U-Sil®5 particles c SEM, particle size distribution scanning electron microscope.

Discussion

In the present study we showed the toxic effect of the ASD in enhancing oxidative stress and disturbing permeability of CALU 3 in a vitro model. We have previously shown that artificial stone dust induced quantitatively functional and inflammatory abnormalities in exposed workers that were bio monitored.[6] Moreover, we further shown that artificial stone dust (ASD) contains high levels of ultrafine particles (UFP <1 µm) which penetrate deeply into the human lungs. This penetration was positively correlated to decrease in the Pulmonary Function Testing, worsening of CT findings and elevation of inflammatory cytokines in the exposed workers.[17]

In this study, we implemented an *in vitro* model utilizing the CALU-3 human alveolar epithelial cell line to investigate the potential toxicity and underlying mechanisms of injury associated with short-term controlled exposure to artificial stone dust.

CALU-3 cells are one of the few respiratory cell lines that form tight junctions *in vitro*, enabling its utility in modeling the airway epithelial barrier in lung research. This attribute renders it a valuable tool for screening ultrafine particles for their capacity to translocate through the pulmonary epithelium.[17–19] It was shown also in other work that initial *in vitro* exposure of human lung epithelial (CALU-3) cells to concentrations ranging from 0 to 300 µg/mL of the ultrafine (<220 nm) fraction of road dust collected from three distinct cities (Lancaster and Birmingham, UK, and Mexico City, Mexico), reveal varying oxidative, cytotoxic, and inflammatory responses.[20] To the best of our knowledge this is the first data using CALU- 3 exposed to ASD.

The surface of artificial stone particles can directly induce oxidative stress, compounded by the release of transition metals from the particles. Ultrafine particles, due to their large specific expansive

a. 37 mg (115mg/cm^2) b. 18.5 mg (57.5 mg/cm^2)

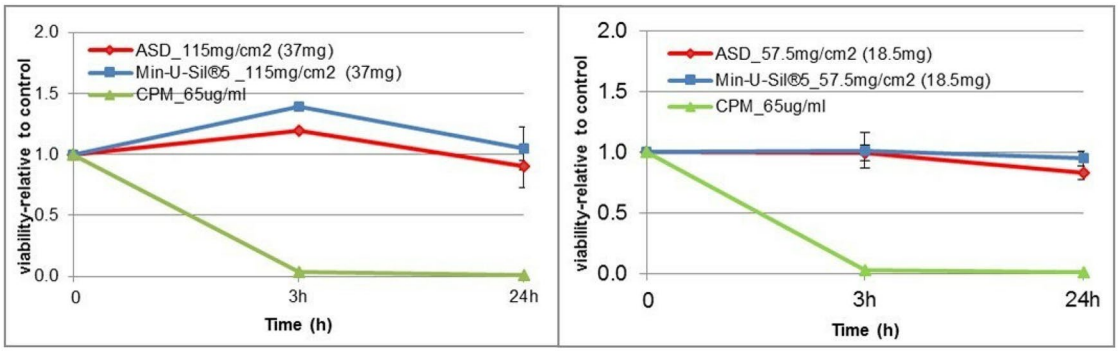

c. 3.7 mg (11.5mg/cm^2)

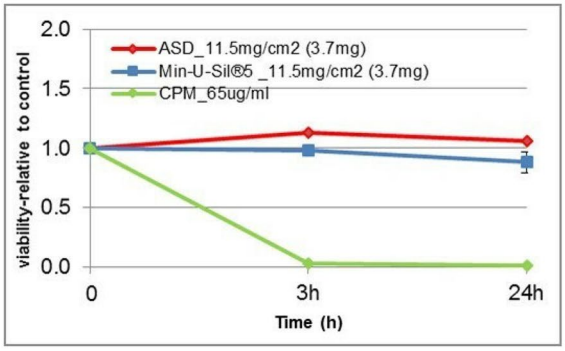

Figure 2. Cell viability CALU-3 cells after 3 h and 24 h exposure to ASD vs Min-U-Sil®5.
Cells grown on 96-well plates for 10 days were treated either with ASD or Min-U-Sil®5 particles and 65µl/ml CPM as positive control. Following exposure, cell viability was measured after 3 and 24 h by Alamar blue assay. Particles concentrations ranged from 11.5 mg/cm^2 to 115 mg/cm^2. The results were expressed relative to control (untreated cells) ± SD of three independent experiments (three replicates each).
ASD, artificial stone dust; Min-U-Sil®5, reference silica particles; CPM, chloropromazine.

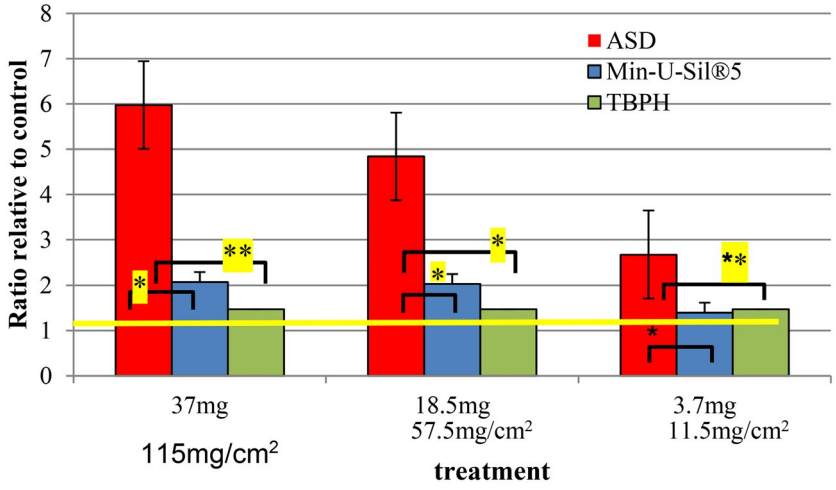

Figure 3. Assessment of oxidative stress after exposure of CALU- 3 cells to ASD vs Min-U-Sil®5.
ASD particles elevated intracellular levels of ROS. Cells were grown in 96-well plates for 10 days, then DCFH-DA was added to the cells for 30 min before the addition of ASD, Min-U-Sil®5, or the positive control 1mM TBPH for an additional 30 hours and 5min for positive control. Particles concentrations ranged from 11.5 mg/cm^2 to 115 mg/cm^2. DCF fluorescence intensity was measured at 485nm excitation and 530nm emission and the results were expressed relatively to control (unexposed cells) ± SD of three independent experiments. Significant statistical difference with respect to the unexposed control (*P < 0.05, **P < 0.01).
ASD, artificial stone dust; TBPH, tetrabutyl per oxyhydroxide, positive control.

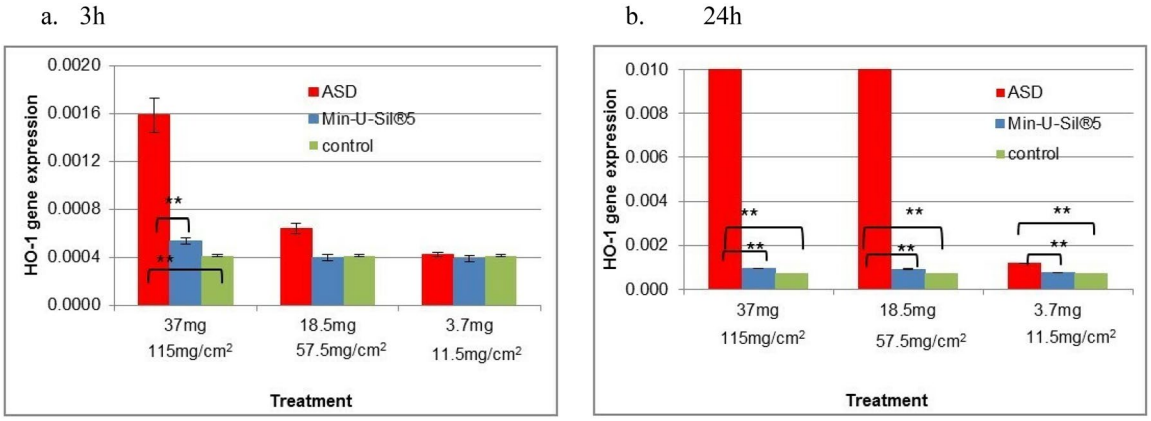

Figure 4. Expression of m RNA in CALU-3 cells of HO-1 Gene Expression following (a) 3 h and (b) 24 h exposure to ASD vs Min-U-Sil®5.

Expression of mRNA levels of HO-1 was done by real time PCR (ΔΔct method) normalized by internal gene (GAPDH). Y axis represents the gene expression relative to GAPDH.

**p value < 0.01 by one-way ANOVA test. The results are ± SE of three independent experiments (three replicates each). ASD, artificial stone dust; HO-1, hemeoxigenase-1.

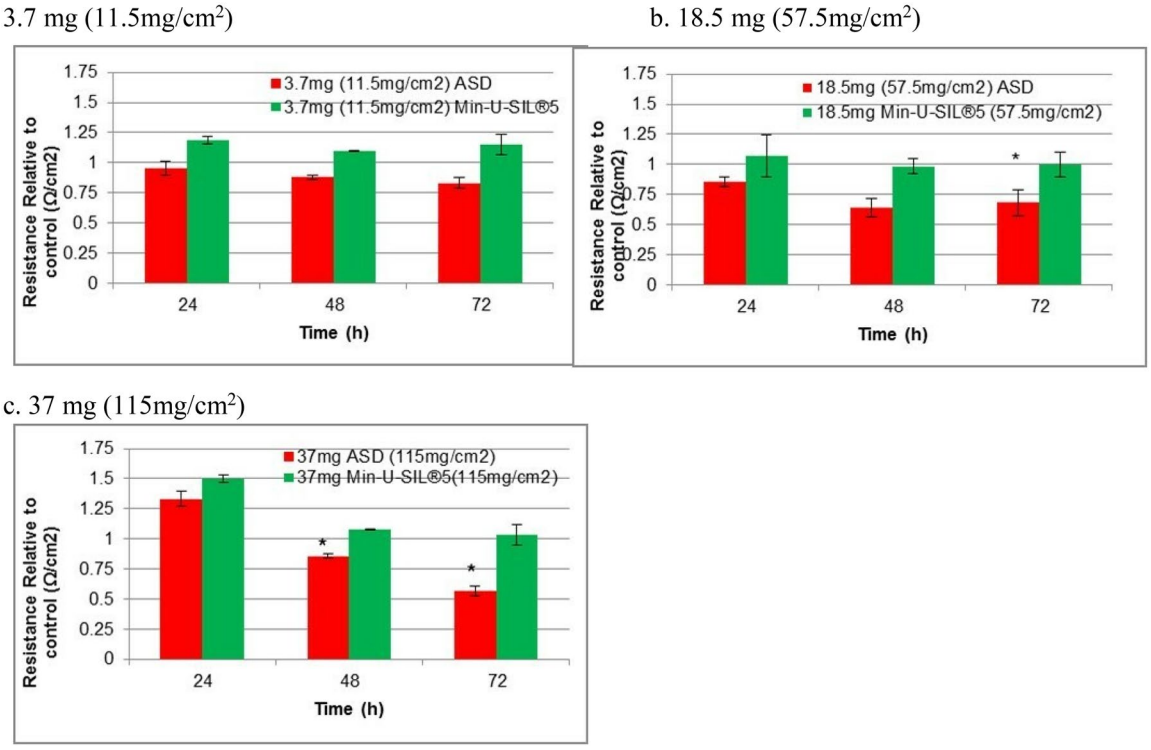

Figure 5. Measurement of transepithelial electric resistance after treatment with ASD and Min-U-Sil®5.

Alteration in TEER in a time and concentration-dependent manner. A–C: Cells grown on 24-transwells for 10 days were treated either with ASD or Min-U-Sil®5 particles. Following exposure, TEER was measured after exposure of cells for 24, 48 and 72 h. Particles concentrations ranged from 11.5 mg/cm² to 115 mg/cm². The results are expressed relatively to control (untreated cells) ± SE of three independent experiments. *Significant difference with respect to Min-U-Sil®5 treatment ($p < 0.05$) by one way ANOVA. ASD, artificial stone dust.

surface area, have the potential to generate significantly more free radicals per unit weight compared to larger particles. This is particularly pronounced in irregular particles formed during mining and drilling processes, as they create reactive surface species.[21] Here, we employed *in vitro* methodology to assess the toxic effects induced by exposure to artificial stone dust (ASD), comparing it with Min-U-Sil®5, that possess a similar size shape characteristics but contains only pure silica. The

artificial stone dust contains other additives like pigments, resins, titanium and polymers that should indicate the more noxious effect of this dust.[2–4]

Our aim was to elucidate the role and action mechanism of ASD exposure on the respiratory tract. To closely replicate human exposure conditions, we determined the average particle concentration in sputum cells of exposed workers (37 mg) and adjusted the ASD and Min-U-Sil®5 concentrations accordingly. The final doses administered were 3.7 mg, 18.5 mg and 37 mg. Notably, none of these concentrations exhibited toxicity to the cells in terms of cell viability

Reactive oxygen species (ROS) are known to play a key role in regulating inflammasomes—large protein complexes that activate inflammatory caspases (such as caspase-1 and caspase-12) and cytokines (including IL-1β and IL-18) in macrophages.[22] Inhaled crystalline silica particles, once phagocytosed in the lungs, cause lysosomal damage that triggers activation of the NALP3 inflammasome, initiating an inflammatory cascade characterized by the release of potent proinflammatory cytokines such as IL-1β and IL-18.[23]

Moreover, many constituents of the nanoparticles are considered toxic or at least hazardous, including polycyclic aromatic hydrocarbons (PAHs) and heavy metal compounds, in addition to gaseous pollutants present in the aerosol fraction, such as NOx, $SO_{2,}$ and ozone. All these compounds can cause oxidative stress, mitochondrial damage, inflammation in the lungs and other tissues, and cellular organelles.[24]

In this context, our investigation focused on examining changes in Reactive Oxygen Species (ROS) generation prompted by ASD demonstrating that ASD led to a heightened ROS level in comparison to Min-U-Sil®5 particles and TBHP. TBHP is a well-established reference agent for inducing ROS in various cell types, tissues, and organisms.[25] Our results demonstrate that both ASD (Artificial Stone Dust) and Min-U-Sil 5 elicit ROS levels far exceeding those induced by TBHP, highlighting their potent oxidative potential in CALU-3 cells. These findings strongly support the likelihood of significant *in vivo* oxidative injury in workers chronically exposed to this dust. Additionally, we observed a substantial elevation in the expression of stress-inducible HO-1gene after a 3-h treatment with the highest dosage studied. This increase remained significant compared to both Min-U-Sil®5 and the positive control oxidizer across all dosages after a 24-h period.

Upregulation of cellular HO-1 levels is a hallmark of oxidative stress due to its subsequent effects, especially under pro-oxidative conditions. In our previous studies, we have demonstrated an increase in HO-1 levels in induced sputum samples obtained from patients afflicted with Chronic Beryllium Disease,[26] as well as in exposed welders.[27] Similar findings have been reported by others in stone carving workers.[28]

Consequently, our results demonstrate an interference of ASD particles with CALU-3 cells in their barrier function, as evidenced by low TEER measurements observed at high ASD concentrations (18.5 mg and 37 mg) after 48 h and 72 h. These TEER values contrast with those obtained for Min-U-Sil®5 at the same concentration and time point. This indicates a significant dysfunction of the epithelial barrier caused by ASD. The weakening of this barrier facilitates the passage of particles through the epithelial cell layer, allowing them to enter the interstitial space, the lymphatic system, and the bloodstream. Consequently, these particles can disseminate to other organs, leading to systemic damage. Maintaining a healthy, intact epithelial barrier with normal gap junction function is essential for reducing the translocation of particles. However, increased epithelial permeability in inflamed airways can lead to greater penetration and translocation of ultrafine particles (UFP) into circulation. Thus, preserving the integrity and functionality of the airway epithelium is vital for lung defense.

The connection between altered oxidative stress and altered gap junctions has been well-demonstrated in various tissues. In the avascular lens, the maintenance of transparency and homeostasis relies heavily on an extensive network of gap junctions. Lens gap junctions, comprised of constituent proteins known as connexins (Cx43, Cx46, and Cx50), are susceptible to the effects of oxidative stress, thereby contributing to the formation of cataracts.[29] Some other proteins such as Tight Junction proteins (JP),[30] Adherents Junction Proteins (AJ)[31] and Membrane Proteins (MP) play a crucial role as well.[32] In pathologies related to the central nervous system (CNS), such as neuroinflammation and oxidative stress, the formation of gap junctions, hemichannels, and pannexons play crucial roles.[33]

The observation that changes in respiratory epithelial permeability alter airways' UFP content had been demonstrated in our previous mice model in which the induction of lung inflammation resulted in a major shift of the UFP pattern toward larger particles, which can be explained by translocation of the smaller

particles into the circulation.[34] Moreover, we observed an outbreak of silica-related autoimmune disease among synthetic stone construction workers with silicosis referred to for lung transplantation assessment.[8]

These cases underscore the strong correlation between silicosis and multiple distinct syndromes of autoimmune diseases.[35] This correlation is further evidenced by the decrease in resistance observed in TEER measurements in our *in vitro* model, as demonstrated here.

The primary limitation of our study lies in its focus on the short-term effects of ASD on epithelial cells, whereas individuals exposed to ASD may experience health implications after prolonged exposure spanning several years. Nonetheless, we posit that our findings elucidate an early event in the cascade of toxic effects associated with ASD exposure.

Another limitation is the use of cell lines, which often lose some of the characteristics of the tissue from which they were derived, potentially reducing their biological relevance.

In conclusion, this study presents, for the first time, the mechanistic pathway through which ASD instigates systemic disorder.

Declaration of interest

No potential conflict of interest was reported by the author(s).

Funding

Committee for Research and Prevention in Occupational Safety and Health in Israel (N0 56/13).

Data availability statement

The authors confirm that the data supporting the findings of this study are available within the article.

References

1. Hoy RF, Jeebhay MF, Cavalin C, et al. Current global perspectives on silicosis—convergence of old and newly emergent hazards. *Respirology*. 2022;27(6):387–398. doi:10.1111/resp.14242.
2. Requena-Mullor M, Alarcón-Rodríguez R, Parrón-Carreño T, Martínez-López JJ, Lozano-Paniagua D, Hernández AF. Association between crystalline silica dust exposure and silicosis development in artificial stone workers. *Int J Environ Res Public Health*. 2021;18(11):5625. doi:10.3390/ijerph18115625.
3. Mandler WK, Qi C, Qian Y. Hazardous dusts from the fabrication of countertop: a review. *Arch Environ Occup Health*. 2023;78(2):118–126. doi:10.1080/19338244.2022.2105287.
4. León-Jiménez A, Mánuel JM, García-Rojo M, et al. Compositional and structural analysis of engineered stones and inorganic particles in silicotic nodules of exposed workers. *Part Fibre Toxicol*. 2021;18(1):41. doi:10.1186/s12989-021-00434-x.
5. Ramkissoon C, Gaskin S, Song Y, Pisaniello D, Zosky GR. From engineered stone slab to silicosis: a synthesis of exposure science and medical evidence. *Int J Environ Res Public Health*. 2024;21(6):683. doi:10.3390/ijerph21060683.
6. Fireman E, Mahamed AE, Rosengarten D, Ophir NN, Kramer MR. Quantitation of silica contents in lung explants of transplanted patients: artificial stone-induced silicosis vs idiopathic pulmonary fibrosis. *Int J Environ Res Public Health*. 2021;18(14):7237. doi:10.3390/ijerph18147237.
7. Ophir N, Shai AB, Alkalay Y, et al. Stone dust-induced functional and inflammatory abnormalities in exposed workers monitored quantitatively by biometrics. *ERJ Open Res*. 2016;2(1):00086-2015. 00086-2015. doi:10.1183/23120541.00086-2015.
8. Shtraichman O, Blanc PD, Ollech JE, et al. Outbreak of autoimmune disease in silicosis linked to artificial stone. *Occup Med (Lond)*. 2015;65(6):444–450. doi:10.1093/occmed/kqv073.
9. Cornwell GC, Sultana CM, Petters MD, et al. Discrimination between individual dust and bioparticles using aerosol time-of-flight mass spectrometry. *Aerosol Sci Technol*. 2022;56(7):592–608. doi:10.1080/02786826.2022.2055994.
10. Zhu J, Hsu CY, Chou WC, et al. PM2.5- and PM10-bound polycyclic aromatic hydrocarbons in the residential area near coal-fired power and steelmaking plants of Taichung City, Taiwan: in vitro-based health risk and source identification. *Sci Total Environ*. 2019;670:439–447. doi:10.1016/j.scitotenv.2019.03.198.

11. Martínez-López A, Candel S, Tyrkalska SD. Animal models of silicosis: fishing for new therapeutic targets and treatments. *Eur Respir Rev*. 2023;32(169):230078. doi:10.1183/16000617.0078-2023.
12. Ramkissoon C, Song Y, Yen S, et al. Understanding the pathogenesis of engineered stone-associated silicosis: the effect of particle chemistry on the lung cell response. *Respirology*. 2024;29(3):217–227. doi:10.1111/resp.14625.
13. Malik M, Steele SA, Mitra D, Long CJ, Hickman JJ. Trans-epithelial/endothelial electrical resistance: current state of integrated TEER measurements in organ-on-a-chip devices. *Curr Opin Biomed Eng*. 2025;34:100588. doi:10.1016/j.cobme.2025.100588.
14. Von Stein BP, Iliadis C. Transcatheter edge-to-edge repair for mitral regurgitation. *Trends Cardiovasc Med*. 2025;35(5):320–325. doi:10.1016/j.tcm.2025.01.014.
15. Schimetz J, Shah P, Keese C, et al. Automated measurement of transepithelial electrical resistance in 96-well transwells using ECIS TEER96: single and multiple time point assessments. *SLAS Technol*. 2024;29(1):100116. doi:10.1016/j.slast.2023.10.008.
16. JEOL USA. Embedded EDS for SEM. JEOL. https://www.jeolusa.com/PRODUCTS/Elemental-Analysis/Embedded-EDS-for-SEM. Accessed September 20, 2025.
17. Ophir N, Bar Shai A, Korenstein R, Kramer MR, Fireman E. Functional, inflammatory and interstitial impairment due to artificial stone dust ultrafine particles exposure. *Occup Environ Med*. 2019;76(12):875–879. doi:10.1136/oemed-2019-105711.
18. Gokse O, Sipahi M, Yanasik S, et al. Comprehensive analysis of resilience of human airway epithelial barrier against short-term PM2.5 inorganic dust exposure using in vitro microfluidic chips and ex vivo human airway models. *Allergy*. 2024;79(11):2953–2965. doi:10.1111/all.16179.
19. Forbes B, Ehrhardt C. Human respiratory epithelial cell culture for drug delivery applications. *Eur J Pharm Biopharm*. 2005;60(2):193–205. doi:10.1016/j.ejpb.2005.02.010.
20. Hammond J, Maher BA, Gonet T, et al. Oxidative stress, cytotoxic and inflammatory effects of urban ultrafine road-deposited dust from the UK and Mexico in human epithelial lung (CALU-3). *Antioxidants (Basel)*. 2022;11(9):1814. doi:10.3390/antiox11091814.
21. Fubini B, Zanetti G, Altilia S, Tiozzo R, Lison D, Saffiotti U. Relationship between surface properties and cellular responses to crystalline silica: studies with heat-treated cristobalite. *Chem Res Toxicol*. 1999;12(8):737–745. doi:10.1021/tx980261a.
22. Wei LY, Xie N, Cai H. Mitochondria-targeted reactive oxygen species blocker SS-31 alleviates hepatic fibrosis by regulating NLRP3 inflammasomes. *Cell Mol Biol (Noisy-le-Grand)*. 2024;70(2):183–188. doi:10.14715/cmb/2024.70.2.25.
23. Zhou H, Zhang Q, Liu C, et al. Inflammasome mediates abnormal epithelial regeneration and distal lung remodeling in silica-induced lung fibrosis. *Int J Mol Med*. 2024;53(3):25. doi:10.3892/ijmm.2024.5349.
24. Portugal J, Bedia C, Amato F, et al. Toxicity of airborne nanoparticles: facts and challenges. *Environ Int*. 2024;190:108889. doi:10.1016/j.envint.2024.108889.
25. Afzal S, Abdul Manap AS, Attiq A, Albokhadaim I, Kandeel M, Alhojaily SM. From imbalance to impairment: the central role of reactive oxygen species in oxidative stress-induced disorders and therapeutic exploration. *Front Pharmacol*. 2023;14:1269581. doi:10.3389/fphar.2023.126958.
26. Kokturk N, Sabag M, Stark M, Grief J, Fireman E. High extracellular induced sputum haem oxygenase-1 in sarcoidosis and chronic beryllium disease. *Eur J Clin Invest*. 2009;39(7):584–590. doi:10.1111/j.1365-2362.2009.02137.x.
27. Stark M, Zubareb J, Jacovovitz A, et al. HO-1 and VEGF gene expressions are time dependent during exposure to welding fumes. *Cytokine*. 2009;46(2):290–295. doi:10.1016/j.cyto.2009.02.012.
28. Thongtip S, Siviroj P, Prapamontol T, et al. A suitable biomarker of effect, club cell protein 16, from crystalline silica exposure among Thai stone-carving workers. *Toxicol Ind Health*. 2020;36(4):287–296. doi:10.1177/0748233720920137.
29. Berthoud VM, Beyer EC. Oxidative stress, lens gap junctions, and cataracts. *Antioxid Redox Signal*. 2009;11(2):339–353. doi:10.1089/ars.2008.2119.
30. Godbole NM, Chowdhury AA, Chataut N, Awasthi S. Tight junctions, the epithelial barrier, and Toll-like receptor-4 during lung injury. *Inflammation*. 2022;45(6):2142–2162. doi:10.1007/s10753-022-01708-y.
31. Kageyama T, Ito T, Tanaka S, Nakajima H. Physiological and immunological barriers in the lung. *Semin Immunopathol*. 2024;45(4-6):533–547. doi:10.1007/s00281-024-01003-y.
32. Du Z, Kan H, Sun J, et al. Molecular mechanisms of acquired resistance to EGFR tyrosine kinase inhibitors in non-small cell lung cancer. *Drug Resist Updat*. 2025;82:101266. doi:10.1016/j.drup.2025.101266.
33. Caruso G, Di Pietro L, Caraci F. Gap junctions and connexins in microglia-related oxidative stress and neuroinflammation: perspectives for drug discovery. *Biomolecules*. 2023;13(3):505. doi:10.3390/biom13030505.
34. Bar-Shai A, Alcalay Y, Sagiv A, et al. Fingerprint of lung fluid ultrafine particles, a novel marker of acute lung inflammation. *Respiration*. 2015;90(1):74–84. doi:10.1159/000430824.
35. Fireman E, Fireman Klein E. Association between silicosis and autoimmune disease. *Curr Opin Allergy Clin Immunol*. 2024;24(2):45–50. doi:10.1097/ACI.0000000000000966.